

Interaction of Compressible Isotropic Turbulence with Expansion Waves: Vorticity Field

Savvas Xanthos*, Minwei Gong* and Yiannis Andreopoulos*

* *Experimental Aerodynamics and Fluid Mechanics Laboratory*

Department of Mechanical Engineering

The City College of the City University of New York

138th and Convent Avenue

New York, New York 10031 USA

ABSTRACT

The interaction of planar expansion waves with homogeneous and isotropic turbulence have been investigated experimentally in the CCNY Shock Tube Research Facility at several Reynolds numbers. In the present configuration the interaction is free from streamline curvature effects, which cause additional effects on turbulence. The flow field was generated by using a variety of rectangular pattern grids of different mesh sizes. The Reynolds number of the flow based on the mesh size, Re_M , ranged from 50,000 to 200,000 while the turbulent Reynolds number Re_λ based on Taylor's microscale was between 180 and 210. A custom made hot-wire vorticity probe was developed capable of measuring the time-dependent highly fluctuating three dimensional velocity and vorticity vectors, and associated total temperature. These measurements allowed for the computations of the vorticity stretching/tilting terms, vorticity generation through dilatation terms, full dissipation rate of kinetic energy term and full rate-of-strain tensor. The effect of expansion waves on damping fluctuations of turbulence was clear. These results indicate that the outcome of the interaction depends strongly on the upstream turbulence of the flow and the attenuation increases in interactions with higher Reynolds numbers.

Introduction

Vorticity is a quantity that can describe viscous effects in a flow field much better than velocity and it is very well suited for defining and identifying organized structures in time-dependent vortical flows because the streamlines and pathlines are completely different in two different inertial frames of reference. In that respect, better understanding of the nature of turbulent structures and vortical motions of turbulent flows, particularly in the high-wavenumber region, often requires spatially and temporally resolved measurements of velocity derivatives.

Lighthill¹ in his wide-ranging introduction to boundary-layer theory provided an extensive description of vorticity dynamics in a variety of flows by using vorticity as a primitive variable for various theoretical considerations. In the past six years an intense effort has been made to extend the techniques developed successfully for measurements of three dimensional vorticity and rate-of-strain tensor in low speed turbulent boundary layers of

Reynolds numbers $Re_\theta=2,700^{2-5}$ and in vortices generated over delta wings⁶ into compressible flows with shock interactions⁷⁻⁹. The measurement of temporally and spatially resolved velocity gradient tensor, $\partial U_i/\partial x_j$, still remains a challenge. In the present work the interaction of isotropic and homogeneous turbulence with expansion waves, shown schematically in Figure 1 has been studied experimentally. In all experiments, the main objective has been to better understand the physics of the interactions and establishing the behavior of the vorticity field.

The interaction of an isotropic and homogeneous turbulent flow with an axisymmetric disturbance, like a normal planar expansion waves is the best paradigm case of a flow where the geometry is reasonably simplified and the basic physics of such interactions can be investigated. Traditionally this flow has been used as a test case where a turbulence model of the LES or RANS class can be evaluated. The absence of turbulence production and the simplified flow geometry can expose the model's strengths and weaknesses.

Detailed experimental investigations of interactions of expansion waves with isotropic turbulence simply do not exist. The only existing studies are rather limited and have been confined to turbulent boundary layers, as it will be discussed shortly.

Past work by many investigators¹⁴⁻¹⁷ has reported direct or indirect evidence demonstrating that in supersonic flow past an expansion corner the boundary layer reverts from turbulent state upstream of the corner to a laminar state downstream. This basically indicates that expansion regions reduce the level of turbulence activity within a compressible boundary layer. This is not unexpected since the boundary layer after the expansion corner encounters a favorable pressure gradient and a strong dilatation effect. In addition streamline curvature over the convex corner also contributes to reduction in turbulence.

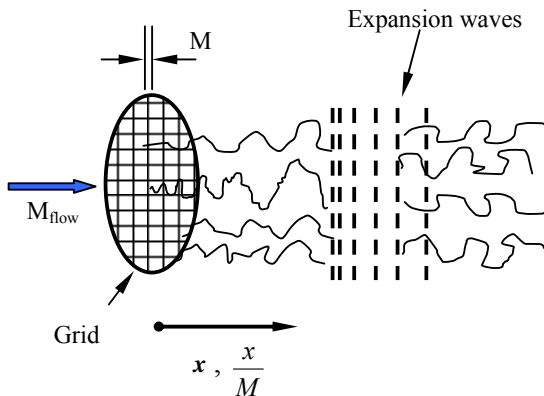


Figure 1: Interaction of expansion waves with homogenous and isotropic turbulence.

Dussauge and Gaviglio¹⁸ studied the rapid expansion of a turbulent boundary layer in supersonic flow both analytically, based on the Rapid Distortion Theory and experimentally emphasizing on the effect of bulk dilatation on turbulent fluctuations. The authors indicated that their Mach 1.76 turbulent boundary layer had been relaminarized by the expansion. Following the same hypotheses as the previously mentioned authors, Smith and Smits¹⁹ used Rapid Distortion Approximation (RDA) to simplify the Reynolds Stress equations, retaining terms, which were then modeled as functions of the Reynolds stress tensor and gradients of the mean flow. Recent work by Arnette, Samimy & Elliot²⁰ and Dawson, Samimy and Arnette²¹ provided more detailed information on the structure of turbulent boundary layers through expansion corners.

Some of the fundamental aspects of turbulence can be studied better in flow configurations where the flow is nearly homogeneous and turbulence is nearly isotropic. The presence of a solid wall as a boundary in turbulent flows complicates its understanding by introducing large mean velocity gradients at the wall which are responsible for the continuous production of turbulence. Better understanding of the effects of shock wave or expansion waves on turbulence, can be obtained by considering their interaction with grid-generated turbulence where no streamline curvature and wall with no-slip conditions are present. The flow behind a turbulence-generating grid contains a large variety of turbulent scales the size of which depends on the distance from the grid and on its mesh size.

Experimental Set-Up and Techniques

The interactions have been simulated experimentally in the CCNY Shock Tube Facility. The shock tube facility is of large scale dimensions with an inside diameter of 12 inches (304 mm) and total length of 90 feet (27.4 m) including all components.

The working (test) section is fitted with several hot-wire and pressure ports. Thus pressure, velocity and temperature data can be acquired simultaneously at various locations downstream from the grid, and therefore reduce the variance between measurements. High frequency pressure transducers, hot wire anemometry and Rayleigh scattering techniques for flow visualization have been used in the present investigation.

A turbulence-generating grid installed in the beginning of the working section of the facility was used to generate a homogeneous and isotropic turbulent flow. The interactions of this flow were generated by using an open end wall of the shock tube, which produces expansion waves when the shock wave is reflected at a lower density interface. "Figure 1" shows schematically the interaction with the expansion waves (EW).

A detailed description of the facility and the results of the qualification tests can be found in the work by Briassulis et al.⁹ and Briassulis¹⁰.

Vorticity Measurements

A new multi hot-wire probe has been developed which is capable of measuring velocity-gradient related quantities in non-isothermal flows or in compressible flows. The present probe has been build upon the experience gained with vorticity measurements in incompressible flows⁴ by using a probe with nine wires, and with velocity measurements in compressible flows by using single and cross-wire probes^{9,12}. The present vorticity probe, which consists of 12 wires, is a modification of the original design with nine wires⁴. The three additional wires were operated in the so-called Constant Current Mode and used to measure time dependent total temperature.

Since the probe essentially consists of a set of three modules or arrays it is necessary to provide several key features of the individual hot-wire modules ("Figure 6"). Each of the 5 μ m diameter tungsten sensors is welded on two individual prongs, which have been tapered at the tips. Each sensor is operated independently since no common prongs are used. Each of the 2.5 μ m diameter cold-wire was located on the outer part of the sub-module.

Extensive testing of the probe has been carried out to assess its performance in shock tube flows. The reader is referred to the work of Briassulis et al.⁸ and Agui et al.⁹ for details of the tests and the techniques associated with the use of the probe. The probe was also tested in low-speed incompressible boundary layer flows where vorticity measurements have been obtained in the past with a 9 wire probe⁴ and with optical techniques¹³. Comparison of the data obtained with the new probe with these previous measurements was very satisfactory.

Velocity calibrations were carried out inside the shock tube by firing the tube at various pressures corresponding to Mach numbers anticipated to be found in the flows under investigation. Yaw and pitch calibration of the probe was also carried out *in-situ*.

Turbulence Modification Through The Interaction With Expansion Waves (EW)

In flows where turbulence is distorted by a rapidly applied

mean shear $S_{11} = \left[\frac{\partial U_1}{\partial x_1} \right]_{\text{Interaction}}$ that is produced by

an expansion wave, the controlling parameter is the ratio

of the time-scale of turbulence $T_\varepsilon = \left[\frac{L_\varepsilon}{q} \right]$ to the time

scale of the applied strain, $\left[\frac{1}{S_{11}} \right]$ i.e. $R_t = \left[\frac{L_\varepsilon S_{11}}{q} \right]$.

L_ε is the dissipative length scale defined as

$L_\varepsilon = \left[\frac{q^3}{\varepsilon} \right]$, q is the square root of the turbulence

kinetic energy $q = \left[\frac{1}{2} \overline{u_i u_i} \right]^{1/2}$ and ε is the dissipation

rate of turbulent kinetic energy q^2 , thus $R_t = \frac{q^2 S_{11}}{\varepsilon}$,

where S_{11} is the strain rate that is associated with the imposed disturbance. In the case of expansion waves interaction it can be approximated by

$$S_{11} = \left(\frac{\partial U_1}{\partial x_1} \right)_{EW} \approx \frac{\Delta U_{EW}}{\Delta x_{EW}}$$

where ΔU_{EW} is the velocity difference across the Expansion Waves and Δx_{EW} is its typical thickness. This can be estimated by $\Delta x_{EW} = \Delta t_{EW} U_C$, where Δt_{EW} is the duration of the expansion zone and $(C - U_2)$ is its convective velocity, which is approximated to be the relative speed of sound in the upstream zone.

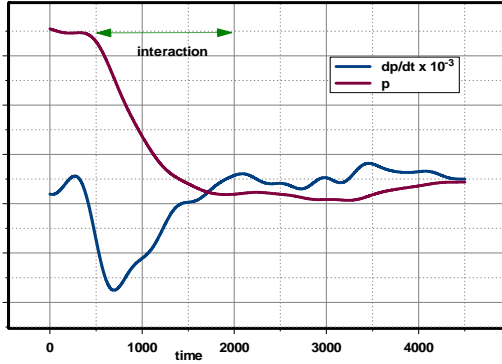


Figure 2: Low-pass filtered pressure signal and its time-derivative.

The time scale ratios, R_t , obtained in the present work are of the order of 10. These data indicate that the imposed disturbance is not as fast as a shock wave although faster than the corresponding eddy turn-over T_e a feature which allows for analysis of data obtained inside the expansion wave. Since the time scales of the expansion wave passage and the time scales of turbulence were reasonably far apart from each other, the data were high-pass and low-pass filtered.

High-pass filtering removed the fluctuations due to turbulence from the signal so that the characteristics of the expansion zone were revealed since they were separated from turbulence. Low-pass filtering removed the low-frequency effects of the expansion waves and only turbulent fluctuations were retained with zero mean. This is called trend removal in signal processing.

A typical result of a low-pass filtering of a wall pressure signal is shown in Figure 2. The interaction zone within the expansion zone is better identified by its derivative dp/dt which is also plotted in the same figure. This time derivative if divided by a typical propagation velocity $C - U$, can be converted to pressure gradient, which is the dominant term in the transport equation. The results show that the pressure gradient peaks very close to the beginning of the interaction region i.e. within 15 percent

of its total duration. Then it starts to relax some of its strength and reaches values close to zero at the end of the duration of the interaction.

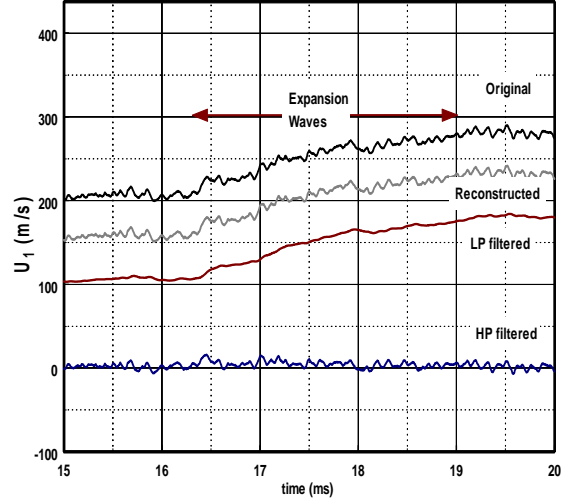


Figure 3: Decomposition of U_1 signal into low- and high-pass filtered contributions. Original and reconstructed signals are shifted by 50 m/s and 100m/s respectively.

Figure 3 shows the decomposition of longitudinal velocity U_1 into its low- and high-pass filtered components, $U_{1,LP}$ and $U_{1,HP}$ respectively. The low-pass component represents the trend in the velocity increase due to the flow acceleration caused by the passage of the EW and it is free of any frequency content above the 500 Hz cut-off value. The HP filtered component does not show low

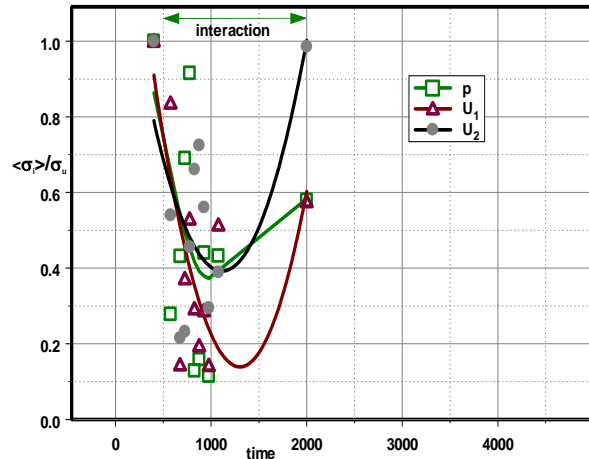


Figure 4: Attenuation of turbulent fluctuations inside the interaction region.

frequency components or trend and it includes the high frequency components of the signal. In order to demonstrate the effectiveness of the decomposition, the two components have been re-combined to form the reconstructed signal $Q_{LP}(t) + Q_{HP}(t) = Q_R(t)$, which as can be seen from figure 3, does not differ from the original signal $Q(t)$.

In order to demonstrate the amplitude of the fluctuations within this interaction, the region was subdivided into ten shorter regions and the r.m.s of the fluctuations was

computed within each of these sub-regions. This information within each of the zone is not an accurate value of the true r.m.s because the process is not stationary. It represents, however, a reasonably good estimate of the amplitude of the fluctuations within each sub-region. These r.m.s values $\langle \sigma_i \rangle$ are normalized by the true r.m.s. value in the upstream region σ_u and are plotted in Figure 4. Thus, the ratio $\langle \sigma_i \rangle / \sigma_u$ indicates the

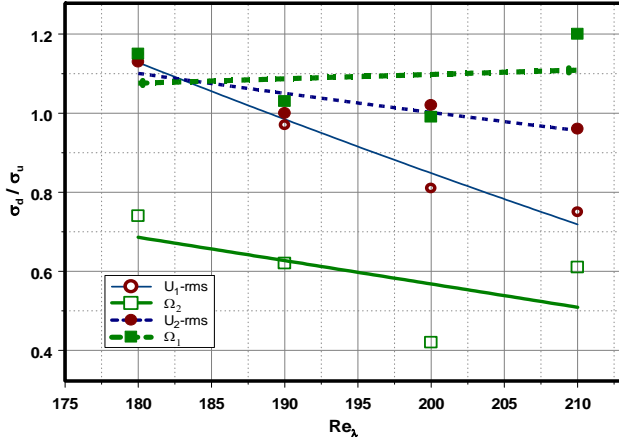


Figure 5: Attenuation of velocity and vorticity fluctuations in expansion wave interactions with turbulence.

attenuation of the fluctuations within the interaction. The data show that fluctuations are attenuated immediately after the start of the interaction and reach the maximum attenuation approximately at the time the pressure gradient reaches its peak value. Then they start to increase and approach the values obtained in the downstream of the interaction region.

Attenuation of turbulence is one of the major features of expansion waves-turbulence interaction. Linear analysis is expected to predict attenuation of turbulence as long as fluctuations of pressure, velocity and temperature upstream of the expansion waves are small so that the front is not substantially distorted and the Rankine-Hugoniot conditions can be linearized. DNS data or other CFD results are not available at this time.

Typically the attenuation of turbulent fluctuations should depend on the expansion waves strength, the state of turbulence of the incoming flow before the interaction, and its level of compressibility.

Figure 5 shows the ratios of the standard deviations $G = \sigma_d / \sigma_u$ for the longitudinal and lateral velocity and vorticity fluctuations. It appears that lateral vorticity fluctuations attenuated the most with ratios between 0.74 and 0.42. The data also show that the attenuations increase with Re_λ . Clear evidence of some attenuation is shown in the data of longitudinal velocity fluctuations, although small amplification has been measured in one experiment. Longitudinal vorticity fluctuations show a constant behavior throughout all Re_λ . Lateral velocity fluctuations show some rather weak dependence on Re_λ . The transmission of the longitudinal vorticity fluctuations through the shock or expansion waves appears to be less affected by the interaction than the fluctuations of the lateral components.

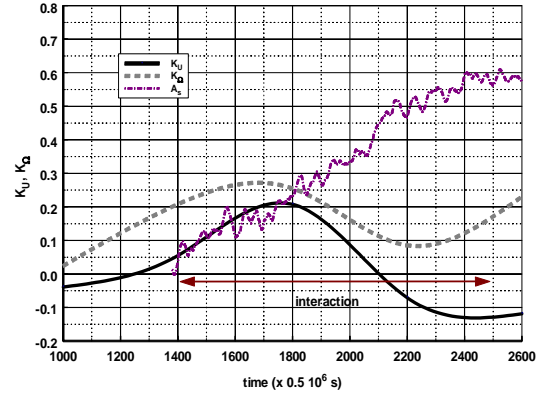


Figure 6: Structural parameter for anisotropy of velocity and vorticity fields.

Departure of isotropy and flow inhomogeneities

The flow homogeneity and isotropy of the upstream flow field has been extensively investigated and documented in Briassulis et. al.⁸ and Agui et. al.^{9,13} In the present interaction which involves an axisymmetric disturbance in the form of a longitudinal straining and an isotropic field, the flow outcome is not expected to be homogeneous and isotropic. In fact some of the turbulence amplification data already indicated departures from isotropy. In order to further explore this behavior, the structural parameters

$$K_U = \frac{\langle \overline{U_1^2} \rangle_{HP} - \langle \overline{U_2^2} \rangle_{HP}}{\langle \overline{U_1^2} \rangle_{HP} + \langle \overline{U_2^2} \rangle_{HP}} \text{ and}$$

$$K_\Omega = \frac{\langle \overline{\Omega_1^2} \rangle_{HP} - \langle \overline{\Omega_2^2} \rangle_{HP}}{\langle \overline{\Omega_1^2} \rangle_{HP} + \langle \overline{\Omega_2^2} \rangle_{HP}} \text{ which indicate the relative}$$

anisotropy of the flow, have been evaluated from the experimental data and plotted in figure 6. The cumulative

straining $A_s(t)$, defined as $A_s(t) = \int_{t_0}^t S_{11}(t') dt'$, has been

also plotted on the same figure. K_U and K_Ω in a purely isotropic flow should be identical to zero. Both parameters maintain relatively low values in the upstream of the interaction. During the early stages of the interaction they reach values close 0.2 and 0.3 respectively and subsequently converge to their residual long term-average values after the interaction, which are higher than their upstream levels. The value of K_U after the interaction is -0.12 which can be considered as border line nearly isotropic flow while the value of K_Ω is 0.24. If these values are compared to the corresponding upstream of the interaction data one can conclude that the isotropy has deteriorated after the interaction. If the flow is homogenous a return to isotropy should be expected through the action of pressure fluctuations. In order to characterize the inhomogeneity of the flow the behavior of the inhomogeneous dissipation, E_b , has been monitored as a function of time. A slow return to isotropy in the present interaction has been found which is in contrast to the fast return to isotropy in the interaction of the present flow with a shock wave (see Agui et. al.^{9,13}). If Rotta's

linear return to isotropy model is considered which describes the rate of change of the normalized anisotropy

tensor b_{ij} defined as $b_{ij} = \frac{\langle u_i u_j \rangle_{HP}}{\langle u_i u_i \rangle_{HP}} - \frac{1}{3} \delta_{ij}$ to be given

by $\frac{db_{ij}}{dt} = -(C_R - 1) \frac{\langle \varepsilon \rangle_{HP}}{\langle q \rangle_{HP}} b_{ij}$ then its solution appears

to be $b_{ij} \sim e^{-(C_R - 1) \langle A_t \rangle}$ which has a decay rate proportional to $\langle A_t \rangle$. The data of this cumulative non-dimensional turbulence indicate that it is a rather weak function of time with a value close to 0.1. In that respect, b_{ij} returns to isotropy rather slowly with time.

Conclusions

The effects of expansion waves interacting with isotropic turbulence have been investigated experimentally. Reynolds numbers based on Taylor's microscale ranging from 180 to 210 have been achieved. The interactions have been investigated by measuring the three-dimensional velocity and vorticity vectors, the full velocity gradient and rate-of-strain tensors with instrumentation of high temporal and spatial resolution. This allowed estimates of dilatation, compressible dissipation and dilatational stretching to be obtained.

The time-dependent signals of enstrophy, vortex stretching/tilting vector and dilatational stretching vector were found to exhibit a rather strong intermittent behavior which is characterized by high amplitude bursts with values up to 8 times their r.m.s. within periods of less violent and longer lived events. Several of these bursts are evident in all the signals suggesting the existence of a dynamical flow phenomenon as a common cause.

Attenuation of longitudinal velocity fluctuations has been observed. It appears that the attenuation increases in interactions with higher Reynolds number. The data of velocity fluctuations in the lateral directions show no change or some minor attenuation through the interaction. These results indicate that the outcome of the interaction depends strongly on the upstream turbulence of the flow.

Acknowledgements

The financial support provided by NASA & AFOSR is greatly acknowledged.

Bibliography

- [1] Lighthill MJ., 1963 "Boundary Layer Theory in Laminar Boundary Layers", (ed. Rosenhead) Oxford University Press.
- [2] Agui JH; Andreopoulos J (1994) Development of a New LASER Vorticity Probe-LAVOR. Fluids Engineering Division of ASME, International Symposium on LASER Anemometry, FED vol. 191, pp. 11-19, editors: Huang, Otugen, Lake Tahoe NV, June 20-24, 1994.
- [3] Agui JH; Andreopoulos Y (2003) A new laser vorticity probe – LAVOR: its development and validation in a turbulent boundary layer. Experiments in Fluids 34: 192-205.

- [4] Hoknan A; Andreopoulos Y (1997a) Vorticity, strain-rate and dissipation characteristics in the near-wall region of turbulent boundary layers. J. Fluid Mech. 350: 29-96.
- [5] Andreopoulos Y; Honkan A (2001) An experimental study of the dissipative and vortical motions in turbulent boundary layers. J. Fluid Mech. 439: 131-163.
- [6] Hoknan A; Andreopoulos Y (1997b) Instantaneous Three Dimensional Vorticity Measurements in Vortical Flow over a Delta Wing. AIAA J. 35(10): 1612-1620.
- [7] Andreopoulos Y; Agui JH; Briassulis G (2000) Shock Wave-Turbulence Interactions. Annu. Rev. Fluid Mech. 32: 309-345.
- [8] Briassulis G; Agui J; Andreopoulos Y (2001) The structure of weakly compressible grid turbulence. J. Fluid Mech. 432: 219-283.
- [9] Agui JH; Briassulis G; Andreopoulos Y (2005) Studies of interactions of a propagating shock wave with decaying grid turbulence: velocity and vorticity field," J. Fluid Mech. Vol. 524, pp. 143-195.
- [10] Briassulis G.K. 1996 *Unsteady Nonlinear Interactions of Turbulence with Shock Waves*. Ph.D. Thesis. City College of CUNY, NY
- [11] Agui, J. 1998 Shock Wave Interactions With Turbulence and Vortices Ph.D. Thesis, City College of CUNY, NY
- [12] G. Briassulis, A. Honkan, J. Andreopoulos and C.B. Watkins, "Application of hot-wire anemometry in shock-tube flows," Experiments in Fluids. 19, 29 (1995).
- [13] Agui J. H., and Andreopoulos Y., "A new laser vorticity probe – LAVOR: its development and validation in a turbulent boundary layer" Exp. Fluids, 34 (2), pp 192-205, 2003.
- [14] Sternberg, J., "The Transition from a Turbulent to a Laminar Boundary Layer," Rept. 906, May 1954, Ballistic Research Labs., Aberdeen, Md.
- [15] Vivekanandan, R., "A Study of Boundary Layer Expansion Fan Interactions near a Sharp Corner in Supersonic Flow," 1963, M.Sc. thesis, Dept. of Aeronautical Engineering, Indian Institute of Science, Bangalore, India.
- [16] Ananda Murthy, K.R. and Hammitt, A. G., "Investigation of the Interaction of a Turbulent Boundary Layer with Prandtl-Meyer Expansion Fan at $M=1.88$," Report 434, 1958, Dept. of Aeronautical Engineering, Princeton University, Princeton, NJ.
- [17] Morkovin, M. V., "Effects of High Acceleration on a turbulent Supersonic Shear Layer," Proceedings, Heat Transfer and Fluid Mechanics Institute, Los Angeles, California, June 1955.
- [18] Dussauge, J.P. and Gaviglio, J. "The rapid expansion of a supersonic turbulent flow: role of bulk dilatation," Journal of Fluid Mechanics, Vol. 174, 1987, pp. 81-112.
- [19] Smith, D.R. and Smits, A. J., "The Rapid Expansion of a Turbulent Boundary Layer in a Supersonic Flow," Theoretical and Computational Fluid Dynamics, 1991 2: 319-328.
- [20] Arnette, S.A., Samimy, M., & Elliott, G.S., 1995, "Structure of Supersonic Turbulent Boundary Layer After Expansion Regions," AIAA Journal, 33, 430-438.
- [21] Dawson, J.D., Samimy, M., & Arnette, S.A., 1994, "The Effects of Expansion on a Supersonic Boundary Layer: Surface Pressure Measurements," AIAA J., 32, No.11, pp. 2169-2177.